Metastability of the uniform magnetization in three-dimensional random-field Ising model systems. I. $Fe_{0.7}Mg_{0.3}Cl_2$

U. A. Leitão and W. Kleemann
Angewandte Physik, Universität Duisburg, D-4100 Duisburg 1, Federal Republic of Germany

I. B. Ferreira*
Max-Planck-Institut für Metallforschung, D-7000 Stuttgart 80, Federal Republic of Germany
(Received 7 March 1988)

The uniform magnetization M of the random-field Ising model system $Fe_{0.7}Mg_{0.3}Cl_2$ was measured using both optical Faraday rotation and superconducting quantum interference device (SQUID) techniques. Thermoremanent magnetization appears after cooling in a field H_0. It follows the relation $\mu \propto H_0^2[T\ln(t/\tau)]^{-1}$ at low temperatures. In close agreement with Nattermann and Vilfan, this describes the spin readjustments within the walls of immobile antiferromagnetic domains. Volume contributions to μ give rise to H_0 dependence of τ. At $T \gtrsim 0.6T_c(H)$, the decay of μ is additionally affected by domain growth. This also causes a decrease of the excess magnetization, ΔM, of the field-cooled domain state after switching the field off and on. Bruinsma-Aeppli-type instantaneous relaxation of ΔM is found in the broad-domain-wall limit very near to $T_c(H)$. $\Delta M > 0$ appears also in a *zero-field cooled* sample upon reversing the T scan *below* T_c within the range of the dynamical rounding. It is attributed to frozen-in fluctuating disorder, which probably does not break the long-range order.

I. INTRODUCTION

It is generally agreed that the random-field Ising model (RFIM) in $d=3$ dimensions undergoes a phase transition into long-range order (LRO).[1] Many aspects of its critical behavior have been elucidated both experimentally[2] and theoretically[3] in the last few years. Unanimity, however, is far from being established. This is partly due to the fact that extreme critical slowing down[3,4] may prevent the system from equilibrating in the critical region. Posssibly, this obscures the true asymptotic critical behavior. On the other hand, due to its extremely slow critical dynamics, the system becomes systematically trapped into a nonequilibrium domain state upon random-field cooling (RFC) through T_c.[5-8]

Experimental evidence of domain states in *ferroic* $d=3$ RFIM systems is rather scarce. Although possible candidates were discussed in the pioneering theoretical work,[9,10] up to now no ferro*magnetic* system containing quenched random fields has convincingly been presented. More probably, some ferro*electric* systems like $K_{1-x}Li_xTaO_3$ containing quenched off-center Li^+ dipoles at $x > 0.022$ seem to exhibit domain states,[11] which have the characteristics of the RFIM in the limit of strain induced Ising symmetry. Furthermore, some structurally disordered systems like $DyAs_xV_{1-x}O_4$ undergoing Ising-like Jahn-Teller phase transitions exhibit typical metastability properties in the RFC state with broken LRO.[12] In all of these cases the LRO of the ground-state can be obtained only after infinitely long relaxation times.[3] Hence, there is no chance at all to study RFIM *critical* behavior in ferroic systems.

A much more favorable situation is met for dilute Ising-type antiferromagnets (AF) exposed to an axial *uniform* field H (DAFF). With respect to their critical behavior they are equivalent to the RFIM.[13,14] By zero-field cooling (ZFC) below $T_c(H)$ and subsequently applying H, one easily achieves the RFIM ground state. Then, upon field-heating (FH) at constant field H one may approach $T_c(H)$ from below and study RFIM critical behavior.[2] On the other hand, upon field-cooling (FC) at constant field H, domain state effects may be studied as well. These manifest themselves at temperatures $T < T_{eq}(H)$, where $T_{eq}(H)$ lies just *above* $T_c(H)$.[2] For example, broadening of the magnetic neutron-diffraction Bragg peaks indicates nondivergence of the order-parameter correlation length as observed on $Fe_{1-x}Zn_xF_2$.[15] Furthermore, one finds smearing of the critical divergences connected with second derivatives of the free energy. The most convincing experiments were, again, first done on the "standard" DAFF system $Fe_{1-x}Zn_xF_2$, using capacitance,[16] linear birefringence,[17] and specific-heat[18] techniques. Logarithmic time dependence, presumably due to domain growth, became manifest only in one of these experiments.[16] Its correspondence to theoretical expectations,[3,5,6] however, is not yet clear.

Metastability of the FC state was also evidenced from measurements of the *uniform* magnetization M of $Mn_{0.6}Zn_{0.4}F_2$ (in the low-field limit)[19] and of $Fe_{0.7}Mg_{0.3}Cl_2$.[20] In accordance with computer simulations,[21] excess magnetization, $\Delta M = M_{FC} - M_{ZFC} > 0$, seems to characterize the FC state at $T < T_{eq}(H)$. The study of $Fe_{0.7}Mg_{0.3}Cl_2$ (Ref. 20) revealed ΔM peaking at $T_m < T_c(H)$, where $T_c - T_m \sim T_{eq} - T_c$, and ΔM_{max} scaling approximately as H^2. This proportionality was related to the expected[5,6] H dependence of the average domain radius, $R \propto H^{-\nu_H}$, where $R \propto \Delta M^{-1}$ and $\nu_H \sim 2$.

The decrease of ΔM for $T < T_m$ was attributed to the decrease of the random fields (RF).

Thermoremanent magnetization (TRM) was recently[22] observed on the DAFF systems $Fe_xMg_{1-x}Cl_2$ with $x=0.45$ and 0.55 after FC. At both of these concentrations, however, spin-glass behavior dominates at low temperatures.[23] Metastability effects due to both spin-glass *and* RFIM properties are, hence, likely to superimpose in a nontrivial manner. Presumably, the coexistence of spin-glass and antiferromagnetic orders as reported by Wong *et al.*[24] on $Fe_{0.55}Mg_{0.45}Cl_2$ reflects this complexity.

In order to clarify the situation, we present investigations on the TRM properties of a RFIM system *without* reentrant spin-glass behavior. This condition is met for the mixture $Fe_{0.7}Mg_{0.3}Cl_2$,[23,24] the ground state of which (after ZFC) corresponds to antiferromagnetic LRO. This is confirmed by the absence of isothermal remanent magnetization (IRM) at all temperatures provided that the threshold field H_c of the metamagnetic phase transition[25] is not exceeded. Hence, the TRM, μ, may be taken as an unequivocal RFIM property of the DAFF system. In the low-T ($T \lesssim T_c/2$) and low-H ($H \ll H_c$) limit our experiments reveal proportionality of μ with H^2. This seems to be compatible with $\mu \propto R^{-1}$, where $R \propto H^{-2}$ is the average domain size.[26] One, hence, concludes that μ, similarly as ΔM,[20] is preferentially concentrated at the domain walls.

Isothermal temporal decay of the TRM as observed in the low-T limit is probably *not* due to domain growth, R versus t, since the FC domain configuration is known[27,21] to be virtually independent of any changes of H, even in the case $H \to 0$. In accordance with recent ideas of Nattermann and Vilfan[28] we presume invariable domain sizes due to random-bond (RB) pinning and relaxation of ΔM by readjustments of the domain walls on fractal length scales. Only at higher temperatures, $T \to T_c$, domain growth seems to contribute to μ versus t.

In that temperature range the excess magnetization, ΔM, of $Fe_{0.7}Mg_{0.3}Cl_2$ has been investigated in more detail. Surprisingly and thus correcting our previous statements,[20] irreversibilities are found in the magnetization curves, M versus T, of both FC *and* ZFC samples. Irreversibility of M_{FC} upon cycling T can be understood by considering domain relaxation due to changes of the RF.[15] In a ZFC sample $\Delta M > 0$ appears upon thermal cycling at temperatures *below*, but *very near* to $T_c(H)$ at constant H. We believe this to be due to freezing of near-critical thermal fluctuations in the range of extreme slowing down of the order-parameter dynamics.[4,5]

It might be questioned, if the metastability of the magnetization as observed on the layered compound $Fe_{0.7}Mg_{0.3}Cl_2$ is a universal feature of *all* DAFF systems. Strong hysteresis of M was also observed on the weakly anisotropic system $Mn_xZn_{1-x}F_2$.[16] However, only very small effects of this kind emerged in the case of $Fe_xZn_{1-x}F_2$ in recent preliminary studies.[29] Since the latter system is considered to be a nearly ideal Ising-like, two-sublattice DAFF system, it seemed to be worthwhile checking its metastability properties in more detail. Indeed, we recently found essentially the same features as for the chloride, utilizing, however, about tenfold stronger fields to obtain effects of the same relative magnitude. The results, obtained on $Fe_{0.47}Zn_{0.53}F_2$, will be presented in a subsequent paper,[30] which will henceforth be denoted as II.

II. EXPERIMENTAL PROCEDURE

All experiments were done on as-cleft samples from a Bridgman-grown boule with nominal composition $Fe_{0.7}Mg_{0.3}Cl_2$. The concentration gradient, $\Delta x/\Delta 1 \sim 0.005$ cm^{-1}, lying within the cleavage plane and perpendicularly to the trigonal **c** axis, was determined by both atomic absorption spectroscopy and measurements of the Néel temperature, T_N, on samples taken from both extremities of the boule. Variations of the Fe^{2+} concentration within about $0.69 \leq x \leq 0.71$ and, hence, variations of the Néel temperatures within 13.4 K $\leq T_N \leq$ 14.2 K were encountered. Since the very hygroscopic crystals usually deteriorate even in the purified He exchange gas of the cryostat, the sample has to be changed whenever warmed up after one experiment. That is why the reported characteristic data like T_N or $T_c(H)$ may be different from one experiment to the other. However, this does not affect the compatibility of the results obtained *within* the course of one particular experiment.

The magnetization, M, was measured either by use of the optical Faraday rotation[31] (FR) or—in the TRM versus t experiments—with a SQUID magnetometer.[32] For the optical measurements strain-free samples with thickness 0.2–0.5 mm were covered with a thin film of paraffin in order to avoid deterioration by moisture. For the same reason small plastic containers sealed with hard paraffin were used to mount the samples with dimensions $2\times2\times0.5$ mm^3 in the SQUID apparatus.

The FR was measured with the apparatus and technique described previously.[20,25] A narrow laser beam (diameter $\sim$0.6 mm, $\lambda = 633$ or 442 nm) probes the sample along its **c** axis. In this configuration the FR is known[33] to be proportional to the parallel magnetization provided the inducing magnetic field is directed along **c**. In the present investigation this was positively confirmed by complementary SQUID measurements. The temperature was stabilized to within $\delta T \sim 1$ mK and the FR angle, θ, was resolved with an accuracy of $\delta\theta = 0.006°$.

III. EXPERIMENTAL RESULTS

A. Remanent magnetization

The TRM, μ, was measured via FR in zero applied field, $H=0$, after cooling the sample within $\Delta t \sim 300$ s from an initial temperature, $T_i \sim 30$ K, through the phase boundary down to the final temperature $T_f \sim 2.8$ K [$T_f < T_c(H_0) < T_N = 14.00 \pm 0.10$ K], at various constant fields, $H_0 = 0.2$, 0.3, 0.4, 0.5, 0.6, and 0.65 T, respectively. In the following H and H_0 denote the fields *during* and—upon FC—*prior to* the measurement, respectively. After stabilization of T_f within $\Delta t \sim 100$ s, H_0 was switched off and the remanent FR was measured on heating in steps of $\Delta t = 0.1$–0.4 K up to $T \sim 20$ K, the delay

time between two measured point being $\Delta t \sim 20$ s. Typical results are presented as θ versus T in Fig. 1(a) for $H_0 = 0.2$, 0.4, and 0.6 T (curves 1, 3, and 5, respectively). After each temperature scan, the sample was ZFC, and FR was registered on heating again. This is shown in Fig. 1(a) by curve 5', which was taken immediately after curve 5. The residual signal is due to the remanent field of the superconducting solenoid, which amounts to 0.2–1 mT, depending on the field used before. As usual for the AF system, the background FR peaks just above T_N in the $H \sim 0$ limit.[33] It is seen that all θ versus T curves in Fig. 1(a) coincide with the background signal (5') at $T \gtrsim 0.9 T_N$.

Figure 1(b) shows the complete set of TRM data, μ versus T, *after* subtracting the background. Curve 3, referring to $H_0 = 0.4$ T, reappears in the inset together with some data points (open circles), each of which involves FC to the respective T, 2.8 K $\leq T < T_N$, and subsequent measurement of the FR at a well-defined time, $t = 20$ s, after switching off the field. Evidently these data fit well with those taken during the thermal scan as described above. We thus conclude that temporal relaxation (see the following) does not sum up during the heating procedure. Hence, all data points displayed in Fig. 1(b) may be taken as equitemporal values $\mu(T,t)$, where $t \sim 20$ s corresponds to the delay-time Δt between successive temperature steps.

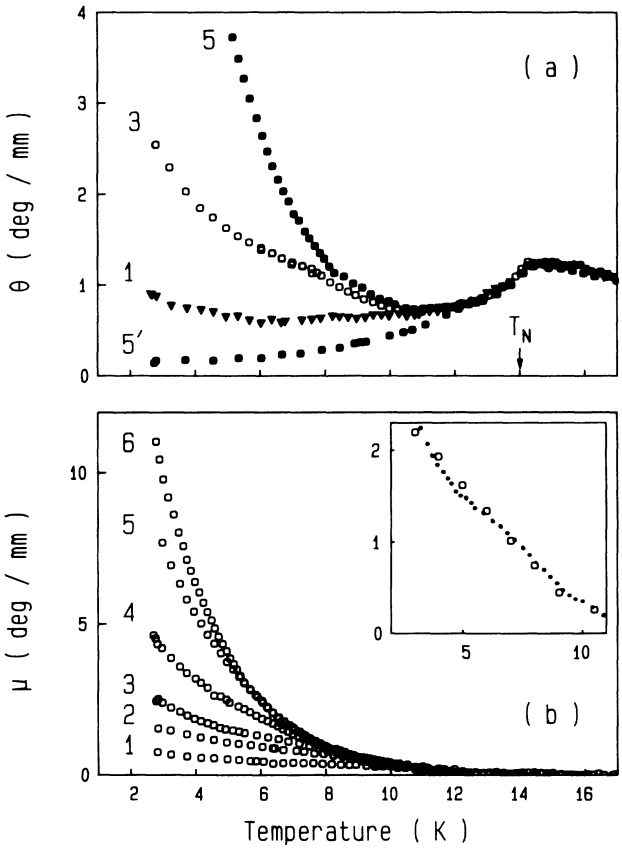

FIG. 1. Temperature dependence of the thermoremanent FR measured on $Fe_{0.7}Mg_{0.3}Cl_2$ with $\lambda = 442$ nm after FC and switching off the field $H_0 = 0.2$ T (curve 1), 0.3 T (2), 0.4 T (3), 0.5 T (4), 0.6 T (5), and 0.65 T (6), respectively. The data are presented, respectively, as θ vs T (a) *before* and as μ vs T (b) *after* subtracting the ZFC background, which is e.g., shown by curve 5' (a) as measured immediately after curve 5 (a). In the inset the μ vs T data of curve 3 (b) (small dots) are compared with those obtained isothermally 20 s after switching off $H_0 = 0.4$ T (open circles).

In order to analyze the data of Fig. 1(b), they are shown in double-logarithmic plots, $\log_{10}\mu$ versus $\log_{10}T$, in Fig. 2. It is seen that power laws,

$$\mu(T) = A_T T^{\nu_T} , \tag{1}$$

are obeyed at low temperatures and in the low-field limit. A least-squares fit of the $H_0 = 0.4$ T curve within 2.8 K $\leq T \leq 7.1$ K yields $\nu_T = -1.00 \pm 0.03$ (solid line in Fig. 2). Similar values, slightly increasing with H_0, are found for adjacent field values, such that $\nu_T = -1.00 \pm 0.10$ might be representative for all $H_0 < H_c$, $H_c(T)$ being the boundary of the AF phase.[25]

Above certain temperatures $T_0(H_0)$ (arrows in Fig. 2), μ is observed to decrease stronger than with T^{-1}. Furthermore, for $T > T_0(H_0)$ all data seem to collapse onto the μ versus T curve obtained after FC with $H \sim H_c$. Clearly, two different relaxation processes seem to govern the T dependence of μ. As will be discussed in Sec. IV A, the T^{-1} regime seems to be related to interface readjustments at virtually constant domain size, $R(H_0)$. At large enough values of H_0 and/or T additional relaxation of μ due to domain growth seems to be superimposed.

It is now interesting to analyze the data of Fig. 1(b) with respect to their H_0 dependence at selected fixed values of T and constant delay-time t (~ 20 s, as previously discussed). Since H_0 determines the domain size of the FC state,[5–8] which very probably[28] does not change upon field quenching, $H \to 0$, in the T^{-1} regime, we expect[20] a simple power law,

$$\mu = A_H H_0^{\nu_H} . \tag{2}$$

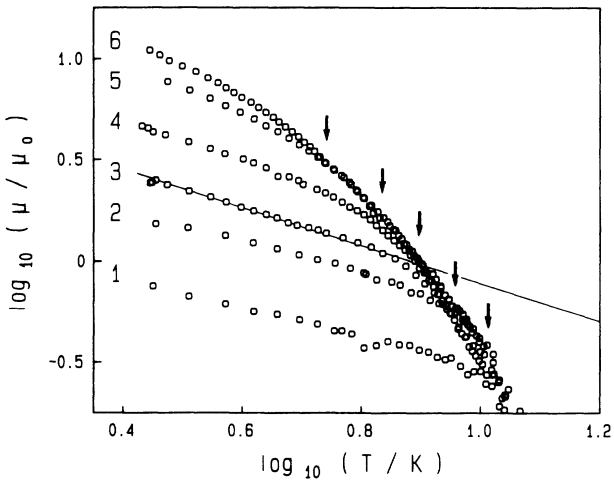

FIG. 2. Double-logarithmic plot of the μ vs T data taken from and identically labeled as in Fig. 1(b) ($\mu_0 = 1$ deg/mm). The solid line is the best fit to Eq. (1) with $\nu_T = -1.00$. Arrows correspond to $T_0(H_0)$ (see text).

Within errors this is indeed the case as shown by log-log plots of μ versus H_0 for $T=3.0$ and 4.0 K in Fig. 3. We find $\nu_H=2.10\pm0.15$. This is essentially confirmed by SQUID data, taken at $T=4.5$ K and $t=80$ s, yielding $\nu_H=1.90$ (open circles). As will be discussed later, this result nicely confirms the expected relations $\mu \propto R^{-1}$ (in analogy to $\Delta M \propto R^{-1}$. Ref. 20) and $R \propto H^{-2}$.[5-8,28]

Temporal decay of μ was observed in both FR and SQUID experiments. Only the latter data will be discussed here, owing to the better long-time stability of the SQUID apparatus. Figure 4 shows μ versus t, measured within 20 s $\leq t \leq$ 8000 s at $T=4.5$ K after FC of the sample in fields $H_0=0.2$, 0.4, 0.6, and 1.2 T. Again, as in the FR experiments (Fig. 1), a non-negligible background due to the remanence of the superconducting solenoid had to be subtracted. This background is exactly reproduced in isothermal remanent magnetization (IRM) experiments, carried out after ZFC, isothermally applying $H<H_c$ for several minutes and subsequently removing H. Curve 5 in Fig. 4 shows the IRM versus t signal referring to $H=0.6$ T and $T=4.5$ K after background correction. It is, hence, concluded that the IRM indeed vanishes throughout the stability range of LRO of the DAFF system obtained after ZFC. However, on application of $H>H_c$ the IRM becomes nonzero. In that case H produces a disordered phase and a domain state evolves upon subsequent field quenching. At high enough fields IRM and TRM become indistinguishable and are essentially determined by the RF corresponding to $H_c(T)$. This is evident from curve 4 in Fig. 4, which was obtained after FC in $H_0=1.2$ T. It closely resembles that corresponding to $H_0=0.6$ T (curve 3), since $H_c=0.66$ T.[25] That is why we shall use an effective field value $H_c=0.66$ T in the evaluation of these data (Fig. 5).

Quite generally[26,28] logarithmic temporal decay is predicted

$$\mu \propto H_0^2[\ln(t/\tau)]^{-\psi}, \tag{3}$$

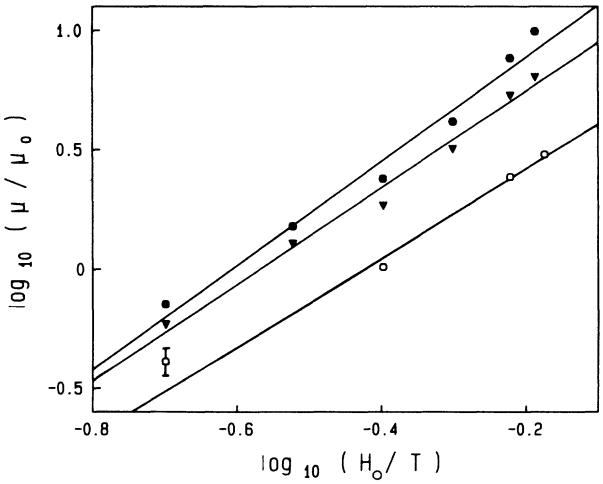

FIG. 3. $\mathrm{Log}_{10}(\mu/\mu_0)$ vs $\log_{10}(H_0/T)$ for $T=3.0$ K (solid circles), 4.0 K (solid triangles), and 4.5 K (open circles), respectively. The solid and open symbols correspond, respectively, to FR ($\mu_0=1$ deg/mm) and to SQUID data ($\mu_0=10^{-3}$ emu). The solid lines are best fitted to Eq. (2) (see text).

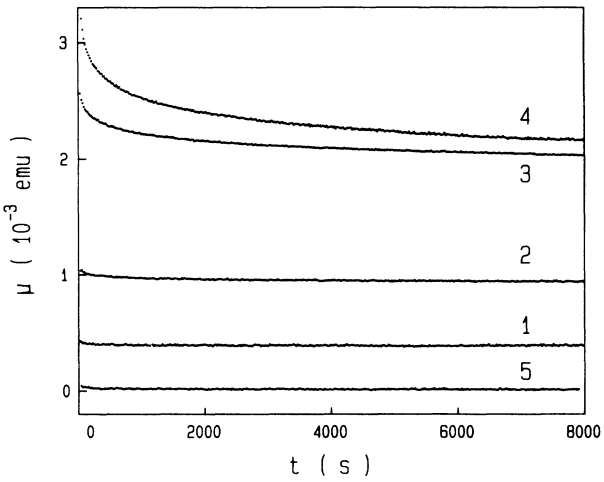

FIG. 4. Time dependence of SQUID TRM data, μ vs t, at $T=4.5$ K after FC in $H_0=0.2$ T (curve 1), 0.4 T (2), 0.6 T (3), and 1.2 T (4), respectively. Curve 5 shows the IRM vs t after ZFC and applying $H=0.6$ T at $T=4.5$ K.

where ψ and τ are some constant and a microscopic spin-relaxation time, respectively. Depending on the temperature range the temporal decay may involve either domain growth[26] ($T \lesssim T_N$) or domain-wall readjustments ($T \ll T_N$).[28] Indeed, semilogarithmic plots, H_0^2/μ versus $\log_{10}t$ (Fig. 5), reveal approximately straight lines, indicating $\psi \sim 1$. Small deviations, observed at $t<100$ s, may be due to incertainties in determining exactly the time zero. Tentatively $t=0$ was set when starting the field decrease. The first data points were thus taken at $t \sim 20$ s.

The attempt times τ, as introduced by relation (3) and determined from the semilogarithmic plots in Fig. 5, are strongly field dependent. Least-squares fits yield $\tau=3\times10^{-22}$, 9×10^{-8}, and 3×10^{-3} s for $H_0=0.4$, 0.6, and 1.2 T, respectively. The relevance of these figures in connection with the proposed[28] relaxation mechanism will be discussed below.

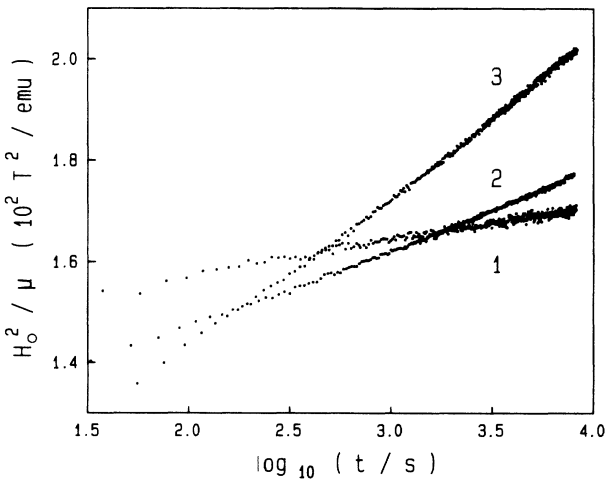

FIG. 5. H_0^2/μ vs $\log_{10}(t/s)$ taken from the data of Fig. 4 for $H_0=0.4$ T (curve 1), 0.6 T (2), and 0.66 T [(3); corresponding to an applied field of 1.2 T (see text)], respectively.

B. Excess magnetization

In order to get more insight into the domain state in nonzero external field, we have studied in some detail the irreversibilities appearing in the magnetization curves (measured via FR) upon cycling both temperature and magnetic field. In Fig. 6(a) we show a typical ZFC-FH-FC cycle for $H=0.5$ T *around* $T_c(H)=11.635(7)$ K (curves 1 and 2). A subsequent FH scan, starting at 11.00 K, is shown by curve 3. It obviously falls *below* the FC curve 2 within 11.00 K $\leq T \leq 11.85$ K. The latter temperature corresponds to $T_{eq}(H)$, below which metastability arises upon FC.[2]

Evidently the FC magnetization, M_{FC}, is *irreversible* in contrast with previous results.[20] These, however, were obtained by cycling in a very limited temperature range, $T_m < T < T_{eq}$, where M_{FC} is, indeed, reversible. Below T_m, however, one observes a monotonic decrease of ΔM,[20] which does not recover upon subsequent heating. The inset of Fig. 6(a) shows $\Delta\theta_{FC}$ peaking at $T_m \sim 11.35$ K and gradually decreasing on lowering T. On heating again, $\Delta\theta_{FH}$ continues to decrease and joins $\Delta\theta_{FC}$ versus T only above $T_{eq}=11.85$ K. We thus conclude that M_{FC} becomes irreversible at low enough T.

Irreversibilities of M_{ZFC} versus T are more subtle to be observed. Figure 6(b) shows several FH-FC cycles performed after ZFC at $H=0.5$ T. Their reversal temperatures, T_r, are indicated by arrows. The lowest cycle is reversible within experimental accuracy. It refers to $T_r=11.52$ K or $\epsilon_r=(T_r-T_c)/T_c=-0.009$. In this case FH and FC data points are collapsing onto curve 1 as expected for the AF ground state of the ZFC configuration. Small, but well-resolved irreversibility, $M_{FC}>M_{FH}$, appears, however, as $T_r \to T_c$. This is evident from the second cycle (curve 2), where $T_r=11.59$ or $\epsilon_r=-0.004$. Here, for the first time metastability *within* the ZFC configuration becomes evident. As will be discussed below, we believe this to be due to pinned near-critical fluctuations on the time scale of the experiment (cooling rate $\sim 10^{-4}$ K/s).

Upon further increasing T_r, ΔM increases until approaching the largest effect at $T_r \geq T_{eq}(H)=11.85$ K (Fig. 6(a), curve 2; Fig. 6(b), curve 5). This is illustrated in Fig. 6(b) by two cycles with $T_r=11.67$ K and 11.79 K (curves 3 and 4, respectively).

Irreversibilities of ΔM introduced by *field cycles* are shown in Fig. 7. The aim of this study was to provide evidence whether or not the FC induced domain structure changes after suppression of the field. First of all the domains were produced by FC in $H_0=0.4$ T, cooling down rapidly ($\Delta t \sim 30$ s) from ~ 20 K to the final temperature, T. By this procedure domain growth at $T \lesssim T_m$ (see above) can largely be avoided and large $\Delta\theta$ signals are preserved (solid circles).[34] After establishing thermal equilibrium, the field was removed and the remanence, μ, was measured after a delay time $t \sim 30$ s (open circles). Then, the field, H_0, was applied again and $\Delta\theta$ registered (solid triangles). Note that after taking one set of isothermal data points the system was heated up to ~ 20 K and the next data set was obtained after another rapid

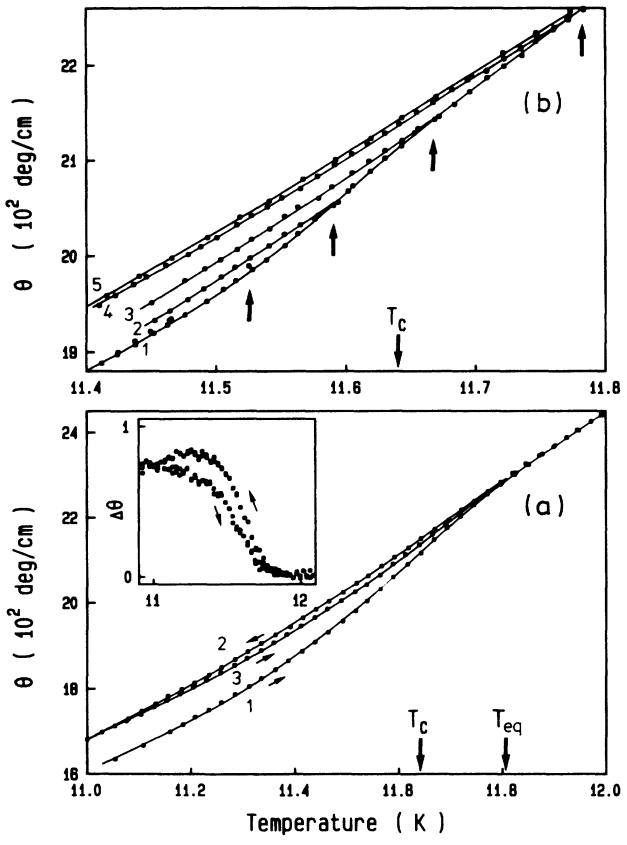

FIG. 6. θ vs T cycles near $T_c=11.64$ K (arrows) measured at $\lambda=633$ nm and $H=0.5$ T. (a) ZFC-FH (curve 1) and FC from above $T_{eq}=11.85$ K (arrow) (2), followed by FH (3) starting at 11.00 K. The inset shows the differences with curve 1 of curves 2 and 3, respectively. (b) ZFC-FH (curve 1) followed by FC after reversing the temperature at T_r (arrows), where $T_r=11.52$ K (FC data collapse with curve 1), 11.59 K (2), 11.67 K (3), 11.79 K (4), and 12.00 K (5), respectively.

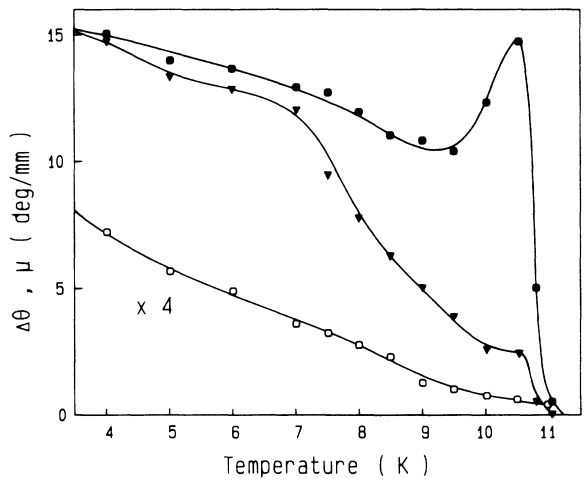

FIG. 7. $\Delta\theta=\theta_{FC}-\theta_{ZFC}$ vs T, measured at $\lambda=442$ nm and $H_0=0.4$ T, where θ_{FC} is determined point by point after rapid FC from 20 K (solid circles) and subsequent removing *and* reestablishing H_0 (solid triangles), respectively. The remanence, μ vs T, measured intermediately at $H=0$ is displayed with a scale factor (open circles). Solid lines are guides for the eye.

FC. Note moreover that the θ_{ZFC} data, needed to calculate $\Delta\theta$ and μ, were measured at both $H=H_0$ and $H=0$ prior to the preceding field cycling procedure.

Most remarkably, $\Delta\theta$ recovers almost completely after sweeping the field through zero and to H_0 again in the low-T range ($T \lesssim 7$ K). This is surprising, since the remanence is as small as $\mu \sim \Delta\theta/10$. Evidently a large fraction of about 90% of $\Delta\theta$ decays very rapidly, but is easily reestablished after creating the RF again via H. However, on increasing T towards T_c [T_c (0.4 T) = 11.01 K in this sample] the loss of $\Delta\theta$ during the field cycle becomes appreciable ($\sim 85\%$ at $0.95T_c$). Very clearly, severe changes of the initial domain structure are now encountered. Decrease of $\Delta\theta$ hints at domain growth and relaxation towards LRO,[16,26] in agreement with our discussion of the μ versus T behavior at $T \rightarrow T_c$ (Figs. 1 and 2).

IV. DISCUSSION

A. Low-temperature relaxation

An FC experiment creates AF domains in a $d=3$ DAFF system, giving rise to the observed excess magnetization, ΔM. Actually, we expect (i) a volume contribution,[28] $\Delta M_v \propto R^{-3/2}$, due to the statistical distribution of the nonmagnetic ions ("vacancies") on both AF sublattices, and (ii) a surface contribution,[20] $\Delta M_s \propto R^{-1}$, because the domain-wall spins are preferentially aligned with H for energetic reasons. For domain sizes $R \sim 200a_0$, say, a_0 being the lattice constant, ΔM_v can be estimated to be no larger than 7% of ΔM_s. Hence, ΔM_v need not be considered in the low-H range, i.e., for large R, except when discussing quantitative details (see the following).

After suppressing the applied field at low T, ΔM relaxes with the time, giving rise to the observed TRM, μ versus t, where $\mu(0)=\Delta M$. For the Ising-like system $Fe_xMg_{1-x}Cl_2$ with strong axial anisotropy ($D/k_B = 17$ K $\sim 30J/k_B$ for $x=1$), the domain walls are narrow at low T and, hence, strongly pinned at the RB.[28] In agreement with neutron scattering[27] and computer simulation data[21] the domain structure is expected[28] to remain frozen in within reasonable laboratory time scales ($t < 10^5$ s). Hence, the observed time dependence of μ cannot be traced back to domain size relaxation as one would expect at the first glance.

As recently pointed out by Natterman and Vilfan,[28] the μ relaxation is rather explained by considering readjustments of the domain walls on short length scales. On small scales, indeed, the ground-state wall configuration is strongly degenerate at $H=0$. It can be achieved from the highly polarized initial state at $H=0$ by small displacements, which effectively decrease ΔM_s, but keep R unchanged. The relaxation is characterized by jumping over local energy barriers. This requires exponentially long times.[28] By applying the field again, the degeneracy is lifted and ΔM will recover, in agreement with the experiments (Fig. 7).

Following Nattermann and Vilfan,[28] relation (3) thus reads at low T

$$\mu(H_0,T,t) = AH_0^2[T\ln(t/\tau)]^{-\psi} , \quad (4)$$

where A and ψ are constants. The H_0 dependence is well verified by the experiment (Fig. 3), yielding $\nu_H = 2.10 \pm 0.15$ in close agreement with the expected value, $\nu_H = 2$. Inspection of the $\log_{10}\mu$ versus $\log_{10}H_0$ plot of Fig. 3 reveals a systematic increase of ν_H for high-field values. This possibly indicates the growing importance of the volume contribution, $\Delta M_v \propto H^3$, at increasing H.

The dependences of μ on both T (Fig. 2) and t (Fig. 5) yield an exponent $-\nu_T \equiv \psi \sim 1$, in disagreement with the theoretically[28] expected value $\psi \sim \frac{2}{5}$. This discrepancy, also found in our relaxation studies of $Fe_xZn_{1-x}F_2$,[30] is yet unsolved. It may be due to still unknown structural properties of the fractal interfaces.[28]

The drastic dependence on H_0 of the decay parameter τ looks problematic at the first glance. Microscopical attempt times are rather expected to be constant and of order 10^{-14}–10^{-10} s. However, as will be shown in more detail in II, the discrepancy is—at least partially—removed, if the volume contribution to μ, $\Delta M_v \propto H_0^3$, is properly accounted for. Most conveniently, Eq. (4) is corrected by introducing a decay parameter τ, which depends on both H_0 and T,

$$\tau = \tau_0 \exp[BH_0T\ln^2(t/\tau_0)] . \quad (5)$$

Here $B>0$ is a constant and τ_0 denotes the microscopic relaxation time. In fact, our results (Sec. III A) indicate an exponential increase of τ with H_0 in agreement with Eq. (5). However, the fitting parameter $\tau_0 \ll 10^{-22}$ s is unphysical.

In order to resolve this discrepancy it appears desirable to check Eq. (5) on μ versus t data of *other* DAFF systems. The much too small value of τ_0 might be an artifact of $Fe_xMg_{1-x}Cl_2$, which is known to exhibit spin-glass properties at $x \lesssim 0.6$.[22–24] Recently, Ferré *et al.*[35] reported TRM versus t data on the 2D-Ising spin-glass $Fe_{0.3}Mg_{0.7}Cl_2$, which resemble very much those displayed in Fig. 4. Hence, one might argue that the spin readjustment *within the* AF *domain walls* of the $x=0.7$ system resemble the spin relaxation in the bulk of systems with $x<0.6$. This seems reasonable, since the domain walls of the RFIM system are known to take advantage of the percolating cluster of nonmagnetic ions. They probe, hence, lower concentrations, $x<0.7$. A stretched exponential function[36,37] as proposed[35] for $x=0.3$ might eventually replace Eq. (4), without, however, providing a clearer insight into the physical relaxation mechanism. A crucial test for detecting different contributions to μ might be measuring its H_0 dependence for $H_0 \rightarrow 0$, being linear and quadratic for spin-glass and RFIM systems, respectively.

B. Relaxation and pinning near $T_c(H)$

In the vicinity of $T_c(H)$ the domain walls are broadened by thermal fluctuations, following the correlation length $\xi \propto |\epsilon|^{-\nu}$.[3,5,38] RB pinning is no longer the leading process.[28] The domain size is rather controlled

by the Bruinsma-Aeppli mechanism[6] and *instantaneously* follows any decrease of the RF, $R \propto H^{-2}$. This is demonstrated by Fig. 7, where switching off the external field essentially yields LRO for $T \lesssim T_c(H)$. This is confirmed by the substantial decrease of $\Delta\theta$ after reestablishing the field H_0.

The decrease of $\Delta\theta$ upon FC below T_m [Fig. 6(a), inset] is, at least partially,[30] also due to a decrease of the RF, which varies essentially as $M(T)/T$.[14] On the other hand, the observed decrease of $\Delta\theta$ upon subsequent FH [Fig. 6(a), inset] is probably *not* due to domain growth. This seems to be excluded in view of recent neutron data on the related system $Fe_{0.6}Zn_{0.4}F_2$.[15] We assume thermally activated domain-wall readjustments in the presence of both RF and RB, hence, $\Delta M \propto T^{-\psi}$ similarly as described by Eq. (4).

We did not explicitly study the time dependence of $\Delta\theta$ at $T \lesssim T_m$.[39] However, neutron data of Wong and Cable[40] on $Fe_{0.7}Mg_{0.3}Cl_2$ hint at isothermal domain growth after FC to $T \sim 0.9T_c(H)$ at $H = 0.45$ T. Moreover, our low-T values of $\Delta\theta$ were observed to depend strongly on the cooling rate through the broad wall regime, $0.8 \lesssim T/T_c(H) < 1$. When stopping FC *within* this temperature range, $\Delta\theta$ drops considerably irrespective of the cooling rate (Fig. 7). Very probably in this intermediate range of T finite domain growth rates are observable, as expected by RFIM theory[3,5,7] and for RB-RFIM systems with intermediate wall widths.[28]

At zero field the immobility of the RB pinned domain walls is only warranted at low T.[28] Thermally activated domain growth will occur at higher temperatures, $T \gtrsim 0.6T_N$ in the present DAFF system. This is evident from enhanced thermal decay of the TRM, $|\nu_T| > 1$, e.g., observed at $T > 7$ K for $H_0 = 0.4$ T (Fig. 2). Furthermore, the substantial decrease of $\Delta\theta$ after suppressing and reestablishing H_0 at $T > 7$ K (Fig. 7) clearly indicates that R is no longer stabilized by RB pinning as $H \to 0$.

The observation of metastability, $\Delta\theta > 0$, in a ZFC sample at $T < T_c(H)$ is probably a dynamical effect. Very near to $T_c(H)$ the RFIM undergoes extreme critical slowing down.[4,26] It causes disordered droplets of size $\xi \propto |\epsilon|^{-\nu}$ to freeze in on a time scale of the order $\tau \propto \exp(\xi^\theta)$, where $\theta \sim 1$.[41] We believe[31,42] that τ approaches the experimental time scale at the critical rounding temperature, ϵ^*. Hence, when reversing a FH scan at $|\epsilon_r| \lesssim \epsilon^*$ the disordered droplets become too sluggish to dissolve on cooling. Enhanced magnetization, typical for the disordered phase, is thus preserved. Very probably, however, it does not percolate thus unaffecting the LRO of the DAFF system.

V. CONCLUSION

Metastability properties of the RFIM system $Fe_{0.7}Mg_{0.3}Cl_2$ were studied in both zero and finite applied fields by FR and SQUID techniques. Our results provide evidence that different mechanisms are responsible for the pinning of field-induced domain walls. RB pinning dominates in the narrow wall low-T limit, whereas the RF mechanism determines the relaxation in the vicinity of $T_c(H)$.

The observed relaxation of the TRM is well described in many aspects by the theoretical model of Nattermann and Vilfan.[28] In particular, the observed time and field dependences are compatible with small scale readjustments of the interfaces. Domain growth is relevant only at higher temperatures, $T \gtrsim 0.6T_c(H)$.

Surprisingly, irreversibility is observed in the long-range ordered state of a ZFC sample upon temperature cycling. It will be interesting to study its interdependence with the critical dynamics using time-resolved measurements. Moreover neutron scattering data are required to prove that LRO is not broken by the frozen-in disorder.

ACKNOWLEDGMENTS

Thanks are due to D. P. Belanger, T. Nattermann, and J. Villain for interesting discussions and suggestions. We are greatly indebted to H. M. Kuss for measuring the concentrations of the mixed crystals. H. Junge helped with the crystal growth. Financial support was provided by the Konrad-Adenauer-Stiftung to one of us (U.A.L.) and by the Deutsche Forschungsgemeinschaft through Sonderforschungsbereich 166.

*Present address: Max-Planck-Institut für Festkörperforschung, D-7000 Stuttgart 80, Federal Republic of Germany.

[1] I. Z. Imbrie, Phys. Rev. Lett. **53**, 1747 (1984).

[2] For recent reviews of the experimental RFIM literature, see R. J. Birgeneau, R. A. Cowley, G. Shirane, and H. Yoshizawa, J. Stat. Phys. **34**, 817 (1984); V. Jaccarino, in *Condensed Matter Physics—The Theodore D. Holstein Symposium,* edited by R. L. Orbach (Springer, New York, 1987), p. 47; D. P. Belanger, Phase Trans. **11**, 53 (1988).

[3] For recent reviews of the theoretical RFIM literature, see J. Villian, in *Scaling Phenomena in Disordered Systems,* edited by R. Pynn and A. Skjeltorp (Plenum, New York, 1985); T. Nattermann and J. Villain, Phase Trans. **11**, 5 (1988).

[4] D. S. Fisher, Phys. Rev. Lett. **56**, 416 (1986).

[5] J. Villain, Phys. Rev. Lett. **52**, 1543 (1984).

[6] R. Bruinsma and G. Aeppli, Phys. Rev. Lett. **52**, 1547 (1984).

[7] G. Grinstein and J. F. Fernandez, Phys. Rev. B **29**, 6389 (1984).

[8] T. Nattermann, Phys. Status Solidi B **129**, 153 (1985).

[9] Y. Imry and S. K. Ma, Phys. Rev. Lett. **35**, 1399 (1975).

[10] A. Aharony, Solid State Commun. **28**, 667 (1978).

[11] W. Kleemann, S. Kütz, and D. Rytz, Europhys. Lett. **4**, 239 (1987).

[12] D. R. Taylor, E. Zwartz, J. H. Page, and B. E. Watts, J. Magn. Magn. Mat. **54 - 57**, 57 (1986).

[13] S. Fishman and A. Aharony, J. Phys. C **12**, L729 (1979).

[14] J. L. Cardy, Phys. Rev. B **29**, 505 (1984).

[15] D. P. Belanger, A. R. King, and V. Jaccarino, Solid State Commun. **54**, 79 (1985).

[16] D. P. Belanger, S. M. Rezende, A. R. King, and V. Jaccarino, J. Appl. Phys. **57**, 3294 (1985).

[17] I. B. Ferreira, A. R. King, and V. Jaccarino (unpublished).

[18]D. P. Belanger (unpublished).
[19]H. Ikeda and K. Kikuta, J. Phys. C **17**, 1221 (1984).
[20]U. A. Leitão and W. Kleemann, Phys. Rev. B **35**, 8696 (1987).
[21]C. M. Soukoulis, G. S. Grest, C. Ro, and K. Levin, J. Appl. Phys. **57**, 3300 (1985); G. S. Grest, C. M. Soukoulis, and K. Levin, Phys. Rev. B **33**, 7659 (1986).
[22]H. Yamashita, K. Iio, M. Sano, H. Masuda, H. Tanaka, and K. Nagata, J. Magn. Soc. Jpn. **11**, Suppl. **1**, 87 (1987).
[23]D. Bertrand, F. Bensamka, A. R. Fert, J. Gelard, J. P. Redoulès, and S. Legrand, J. Phys. C **17**, 1725 (1984).
[24]P. Z. Wong, S. von Molnar, T. T. M. Palstra, J. A. Mydosh, H. Yoshizawa, S. M. Shapiro, and A. Ito, Phys. Rev. Lett. **55**, 2043 (1985).
[25]U. A. Leitão and W. Kleemann, J. Magn. Soc. Jpn. **11**, Suppl. **1**, 95 (1987).
[26]J. Villain, J. Phys. (Paris) **46**, 1843 (1985).
[27]M. Hagen, R. A. Cowley, S. K. Satija, H. Yoshizawa, G. Shirane, R. J. Birgeneau, and H. J. Guggenheim, Phys. Rev. B **28**, 2602 (1983); R. A. Cowley, H. Yoshizawa, G. Shirane, and R. J. Birgeneau, Z. Phys. B **58**, 15 (1984).
[28]T. Nattermann and I. Vilfan, Phys. Rev. Lett. **61**, 223 (1988).
[29]W. Kleemann (unpublished).
[30]P. Pollak, W. Kleemann, and D. P. Belanger, the following paper, Phys. Rev. B **38**, 4773 (1988).
[31]W. Kleemann, A. R. King, and V. Jaccarino, Phys. Rev. B **34**, 479 (1986).
[32]SHE Company (San Diego, Calif.), model VTS.
[33]U. A. Leitão and W. Kleemann, Europhys. Lett. **5**, 529 (1988).
[34]The most perfect method to obtain maximum $\Delta\theta$ at H and T involves isothermal field quenching from H_0 to $H(H_0 \gg H)$ (see also Ref. 30).
[35]J. Ferré, J. Pommier, and D. Bertrand, J. Magn. Soc. Jpn. **11**, Suppl. **1**, 83 (1987).
[36]H. Yoshizawa and D. P. Belanger, Phys. Rev. B **30**, 5220 (1984).
[37]A. T. Ogielski, Phys. Rev. B **32**, 7384 (1985).
[38]B. Widom, J. Chem. Phys. **43**, 3892 (1965).
[39]At $T_m \leq T \leq T_{eq}$ time dependence of $\Delta\theta$ seems to be absent (see Ref. 20.)
[40]P. Z. Wong and J. W. Cable, Phys. Rev. B **28**, 5361 (1983).
[41]A. T. Ogielski and D. A. Huse, Phys. Rev. Lett. **56**, 1298 (1986).
[42]A. R. King, J. A. Mydosh, and V. Jaccarino, Phys. Rev. Lett. **56**, 2525 (1986).